

Supporting Information

Ionic liquid-based synthesis of MXene

Samantha Husmann,¹ Öznil Budak,^{1,2} Hwirim Shim,^{1,2} Kun Liang,⁴ Mesut Aslan,¹

Angela Kruth,³ Antje Quade,³ Michael Naguib,⁴ Volker Presser^{1,2,*}

¹ INM - Leibniz Institute for New Materials, Campus D2 2, 66123, Saarbrücken, Germany

² Department of Materials Science and Engineering, Saarland University, Campus D2 2, 66123, Saarbrücken, Germany

³ Leibniz Institute for Plasma Science and Technology, 17489, Greifswald, Germany

⁴ Department of Physics and Engineering Physics, Tulane University, New Orleans, Louisiana 70118, United States of America

* Corresponding author's e-mail: volker.presser@leibniz-inm.de

1. Experimental Section

1.1 Chemicals

The following chemicals were used without prior purification: two different Ti_3AlC_2 phases were utilized. One was purchased from Kai Kai (denoted KK, Laizhou Kai Kai, 99% purity, $< 25\ \mu\text{m}$), and the other was synthesized from elemental powders and denoted TU (Tulane University) by mixing titanium, aluminium, and graphite (atomic ratio of $3\text{Ti}+1.2\text{Al}+1.88\text{C}$) for 3 h with the aid of yttrium stabilized zirconia balls in a Turbula T2F mixer at 56 rpm, then heated to 1600°C and held for 4 h in a tube furnace with a continuous flow of argon. After letting the sample cool down to room temperature, it was ground and sieved, then only $< 44\ \mu\text{m}$ powder was used afterward. Ti_2AlC (Laizhou Kai Kai), 1-Ethyl-3-methylimidazolium tetrafluoroborate (EMIMBF_4 , IOLITEC), 1-butyl-3-methylimidazolium hexafluorophosphate (BMIMPF_6 , IOLITEC), carbon black (C65, IMERYS Graphite&Carbon), polyvinylidene fluoride (PVDF, Sigma Aldrich), N-methyl-2-pyrrolidone (NMP, Sigma Aldrich), 1 M lithium hexafluorophosphate (LiPF_6) in ethylene carbonate and dimethyl carbonate (EC:DMC; 1:1 by volume; Sigma Aldrich).

1.2 MAX etching

The MAX etching was performed in a Teflon reactor with a 2 mm hole opening in the lid centre for pressure/ gas release. The MAX phase (180 mg) was mixed with the ionic liquid (10 mL) and water and stirred for 20-44 h at 80°C (oil bath), according to **Table S1**. The argon atmosphere was done by constantly bubbling argon in the mixture through a connection in the lid. For synthesis number 7, the whole process was performed inside a glove box due to the absence of water in the system. After the reaction time, the mixtures were filtrated and washed with Milli-Q water using a paper filter. For synthesis number 3, the reaction was filtrated after 22 h, and the powder added to a fresh mixture of water and IL for another 22 h, denominated double etch (DE). The powder was then centrifugated and washed with Milli-Q water until pH 6 (three washes of 30 min at 6000 rpm) and then washed twice with acetone. The powder was dried overnight (ca. 12 h) at 80°C and kept in an Argon-filled glovebox (O_2 , $\text{H}_2\text{O} < 1\ \text{ppm}$). The filtrated liquid was dried overnight at 80°C to partially remove water from reaction and pre-concentrate IL residue. The remaining liquid was centrifugated for 30 min at 6000 rpm. The liquid was separated and denominated IL residue. The remaining powder was washed and centrifugated (30 min at 600 rpm) 3 times with Milli-Q water and twice with acetone.

For comparison with the standard etching method, 1 g of Ti_3AlC_2 powder (from Tulane University) was etched in 10 mL aqueous hydrofluoric acid (HF, 48 to 51% solution in water, Acros Organics, USA) solution for 24 h with stirring at 25°C . After etching, the mixture was centrifuged at 3500 rpm for 3 minutes to separate the sediments. The supernatant was discarded and replaced by degassed deionized water. These steps were repeated until the pH of supernatant reached $\sim 6-7$. All the samples were dried overnight by a vacuum-assisted suction filtration process. The sample was named $\text{Ti}_3\text{C}_2\text{T}_x\text{-HF}$.

Table S1: List of samples produced in different IL etching conditions.

	Synthesis	Sample	MAX/source	IL	IL:W	t (h)	Atmosphere
Ti ₃ AlC ₂	1	Ti ₃ C ₂ T _x	Ti ₃ AlC ₂ /TU	EMIMBF ₄	1:3	20	Air
	2	Ti ₃ C ₂ T _x -K	Ti ₃ AlC ₂ /KK	EMIMBF ₄	1:3	20	Air
	3	Ti ₃ C ₂ T _x -DE	Ti ₃ AlC ₂ /TU	EMIMBF ₄	1:3	<u>2x22</u>	Air
	4	Ti ₃ C ₂ T _x -44h	Ti ₃ AlC ₂ /TU	EMIMBF ₄	1:3	<u>44</u>	Air
	5	Ti ₃ C ₂ T _x -Ar	Ti ₃ AlC ₂ /TU	EMIMBF ₄	1:3	20	<u>Argon</u>
	6	Ti ₃ C ₂ T _x -44hAr	Ti ₃ AlC ₂ /TU	EMIMBF ₄	1:3	<u>44</u>	<u>Argon</u>
	7	Ti ₃ C ₂ T _x -(1:0)	Ti ₃ AlC ₂ /TU	EMIMBF ₄	<u>1:0</u>	20	<u>Argon</u>
Ti ₂ AlC	8	Ti ₂ CT _x	Ti ₂ AlC/KK	EMIMBF ₄	1:3	20	Air
	9	Ti ₂ CT _x -PF ₆	Ti ₂ AlC/KK	<u>BMIMPF₆</u>	1:3	20	Air
For all syntheses: MAX mass: 180 mg, volume of IL: 10 mL; temperature: 80 °C. TU: Tulane University, KK: Kai Kai, EMIMBF ₄ : 1-ethyl-3-methylimidazolium tetrafluoroborate, BMIMPF ₆ : 1-butyl-3-methylimidazolium hexafluorophosphate							

1.3 Material characterization

Scanning electron microscopy (SEM) and energy dispersive X-ray analysis (EDX) was carried out using a JEOL JSM-7500F system coupled to an Oxford Instruments EDX detector with an acceleration voltage of 3 kV for imaging and 15 kV for spectroscopy. The samples were mounted and analysed without any conductive sputter coating.

Transmission electron microscopy (TEM) was performed using a JEOL 2100F system at an acceleration voltage of 200 kV. The samples were dispersed in ethanol through tip sonication for 30 s, drop-casted onto a copper grid coated with a lacey carbon film, and dried at room temperature overnight.

X-ray diffraction (XRD) was conducted with a D8 Discover diffractometer (Bruker AXS) with a copper source (Cu-K α , 40 kV, 40 mA), a Göbel mirror, and a 1 mm point focus. A two-dimensional VANTEC-500 detector covered an angular range of 20° 2 θ with frames recorded at 20°, 40°, 60°, and 80° 2 θ using a measurement time of 720 s per frame, with a beam knife placed over the sample holder.

Raman spectra were acquired with a Renishaw inVia Raman microscope with an Nd-YAG laser of 532 nm excitation wavelength at 0.2 mW power. The spectra were recorded on at least 15 points for each sample, with 20 s acquisition time for 10 accumulations using an objective lens with a numeric aperture of 0.75. Spectra fitting and deconvolution was done with four Voigt peaks. The data shown here is a representative spectrum.

X-ray photoelectron spectroscopy (XPS) was performed with an Axis Supra (Kratos Analytical) spectrometer. Wide and elemental scans were acquired employing Al-K α radiation with 225 W power with a pass energy of 160 eV and 80 eV, respectively, while for high-resolution measurements, 225 W with 10 eV were used. The data processing was done with CasaXPS (Casa Software, version 2.3.15).

2.4 Electrochemical characterization

For electrochemical testing, the etched samples were coated over Cu foil (MTI corporation). The electrode was prepared with 80 mass% active material ($\text{Ti}_3\text{C}_2\text{T}_x$ or $\text{Ti}_3\text{C}_2\text{T}_x\text{-K}$), 10 mass% carbon black (type C45), and 10 mass% PVDF. NMP was added dropwise to the mixture until slurry achieved proper viscosity. The slurry was doctor-blade casted with a wet thickness of 200 μm . The coated electrodes were kept in the fume hood for one day, and vacuum dried at 100 $^\circ\text{C}$ for 12 h. For the characterization, the materials were assembled in a three-electrode setup using polyether ketone (PEEK) cells.^{1, 2} Discs of 8 mm diameter were punched from the coating and used as working electrodes (WE). The average active mass loading values of electrodes were 8.35 mg/cm^2 , 3.90 mg/cm^2 , and 0.81 mg/cm^2 for $\text{Ti}_3\text{C}_2\text{T}_x\text{-HF}$, $\text{Ti}_3\text{C}_2\text{T}_x$ and $\text{Ti}_3\text{C}_2\text{T}_x\text{-K}$, respectively. A lithium metal disc of 11 mm diameter was used both as the counter electrode (CE) and a reference electrode (RE). A glass fibre (GF/D, Whatman) and a Celgard 2325 discs of 13 mm diameter were used as separators between WE and CE/RE, being the Celgard on the CE/RE side. The partially assembled cells were dried in a vacuum oven at 120 $^\circ\text{C}$ for 12 h and then transferred to an argon-filled glove box, where the lithium electrode was introduced and the 1M LiPF_6 in EC:DMC electrolyte backfilled with a syringe. Cyclic voltammetry (CV) and was performed with a potentiostat/galvanostat VMP300 (Bio-Logic) operated with EC-Lab software. Cyclic voltammograms were recorded at a rate of 0.2 mV/s for 10 cycles between 0.01 V and 2.5 V vs. Li/Li^+ . Galvanostatic cycling with potential limitations (GCPL) was done in an Arbin Battery Cycler in a potential range of 0.01 V to 2.5 V vs. Li/Li^+ at current rates of 50-2000 mA/g. For the calculation of the specific current and specific capacity, the mass of active material was used for normalization.

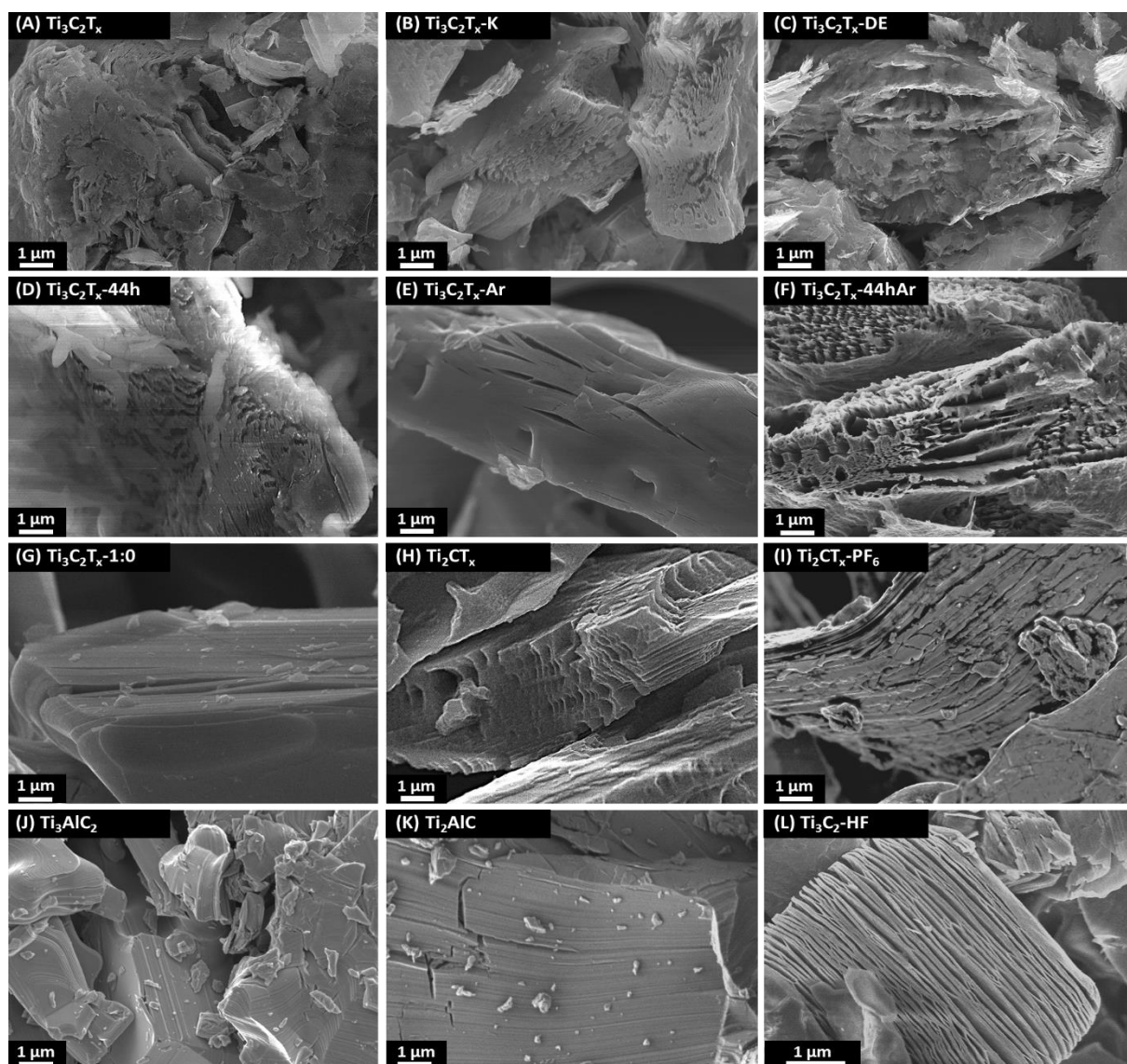


Figure S1: Scanning electron micrographs of the MAX phases etched with EMIMBF₄ and BMIMPF₆ in different synthetic conditions (A-I) and before treatment (J,K). Standard HF-treated sample (L).

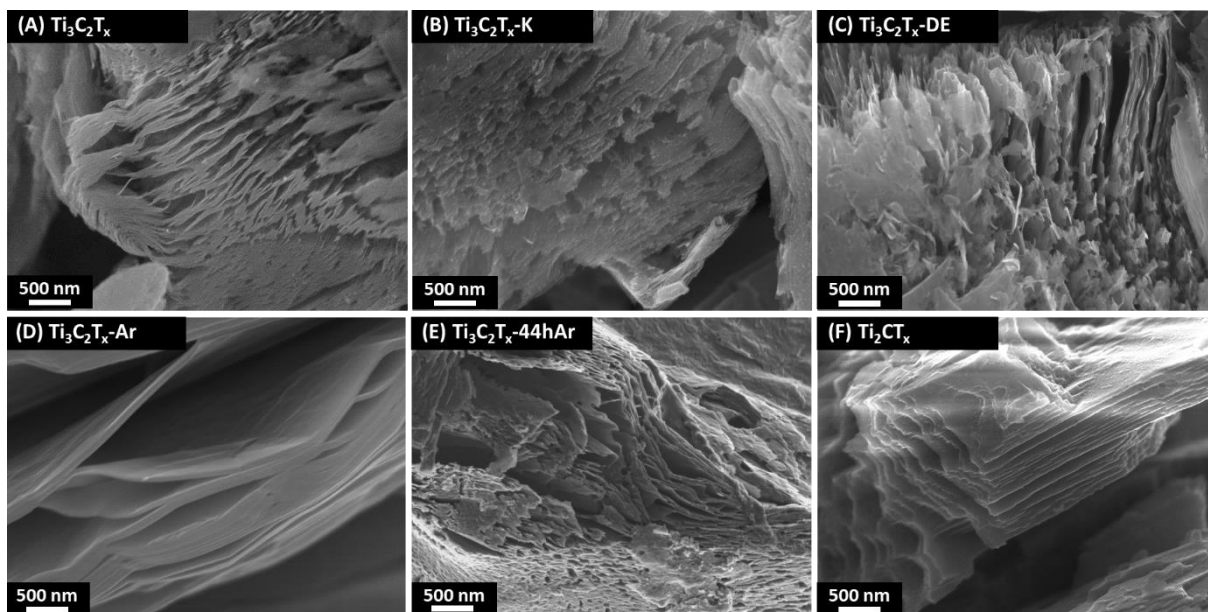


Figure S2: Scanning electron micrographs at higher magnification of the MAX phases etched with EMIMBF₄ in the most efficient synthetic conditions.

Table S2: Energy-dispersive X-ray spectroscopy result regarding elemental composition in at%. The values were normalized to Ti at% being 3 in Ti₃AlC₂ and 2 in Ti₂AlC.

Sample	C	O	F	Al	Ti
Ti ₃ AlC ₂	2.4±0.5	0.4±0.2		1.1±0.1	3.0±0.5
Ti ₃ AlC ₂ -K	2.4±0.5	0.3±0.1		1.0±0.1	3.0±0.5
Ti ₃ C ₂ T _x	1.8±0.5	1.2±0.6	0.7±0.5	0.1±0.2	3.0±1.2
Ti ₃ C ₂ T _x -K	3.2±0.3	2.4±0.5	0.8±0.2	0.1±0.1	3.0±0.8
Ti ₃ C ₂ T _x -DE	3.1±0.9	2.4±0.9	1.0±0.7	0.3±0.2	3.0±1.6
Ti ₃ C ₂ T _x -44h	3.2±1.9	4.4±1.2	3.9±2.2	1.0±1.0	3.0±2.1
Ti ₃ C ₂ T _x -Ar	2.4±0.9	1.3±0.6	0.5±0.3	0.3±0.3	3.0±1.6
Ti ₃ C ₂ T _x -44hAr	0.7±0.4	0.6±0.5	0.5±0.8	0.3±0.7	3.0±1.3
Ti ₃ C ₂ T _x -1:0	2.3±0.9	0.6±0.6	0.3±0.2	0.9±0.5	3.0±1.2
Ti ₂ AlC	1.0±0.3	0.4±0.1		0.9±0.4	2.0±0.6
Ti ₂ CT _x	1.5±0.5	0.5±0.3	0.5±0.4	0.6±0.3	2.0±0.7
Ti ₂ CT _x -PF ₆	1.5±0.5	0.4±0.1	0.2±0.1	0.9±0.3	2.0±0.9
Ti ₃ C ₂ T _x -HF	2.6±0.1	1.7±0.2	3.4±0.2	0.1±0.0	3.0±0.1

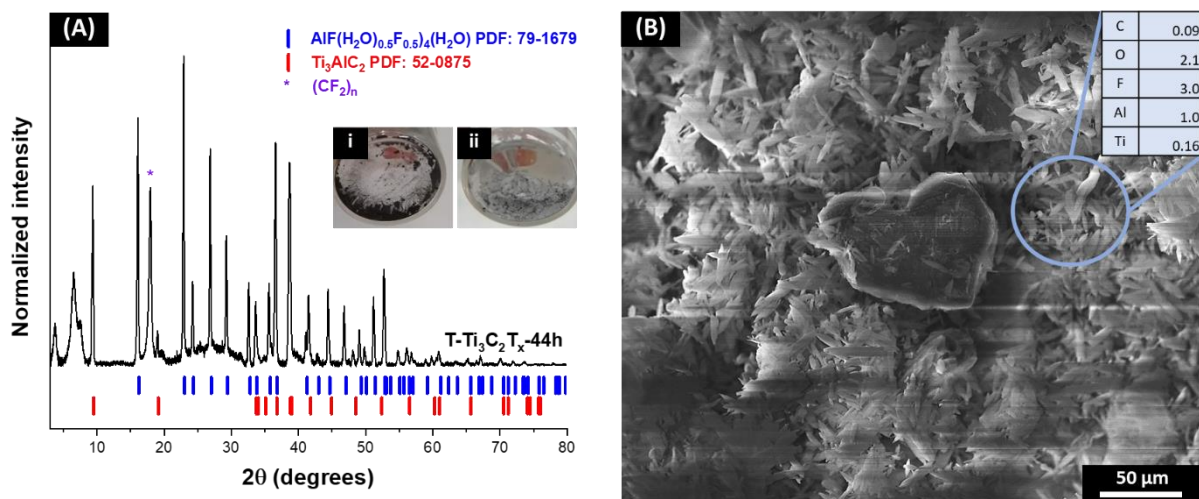


Figure S3: Characterization of $\text{Ti}_3\text{C}_2\text{T}_x\text{-44h}$ sample showing AlF_3 contamination. (A) XRD and (B) SEM images with EDX data inset (normalized to Al atomic% as being 1). Digital photographs of the MAX etched for (i) 20 h and (ii) 44 h.

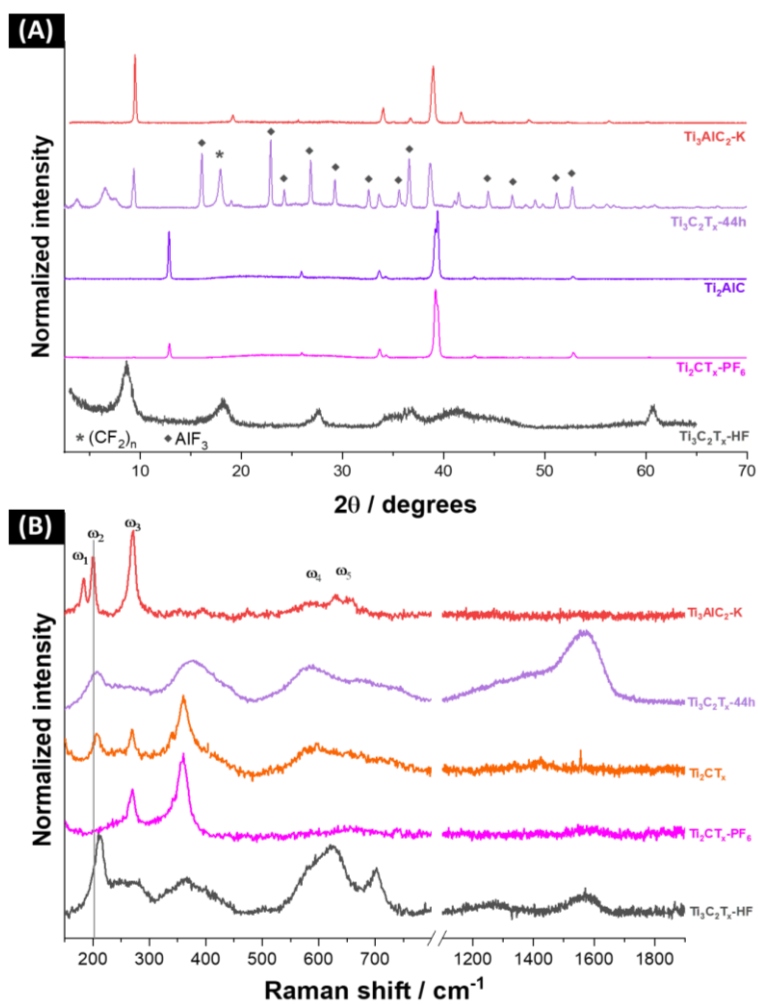


Figure S4: (A) X-ray diffraction patterns ($\lambda=0.154$ nm) and (B) Raman spectra ($\lambda=532$ nm) from the MAX phases and after different treatments with ionic liquid and HF-etched for comparison.

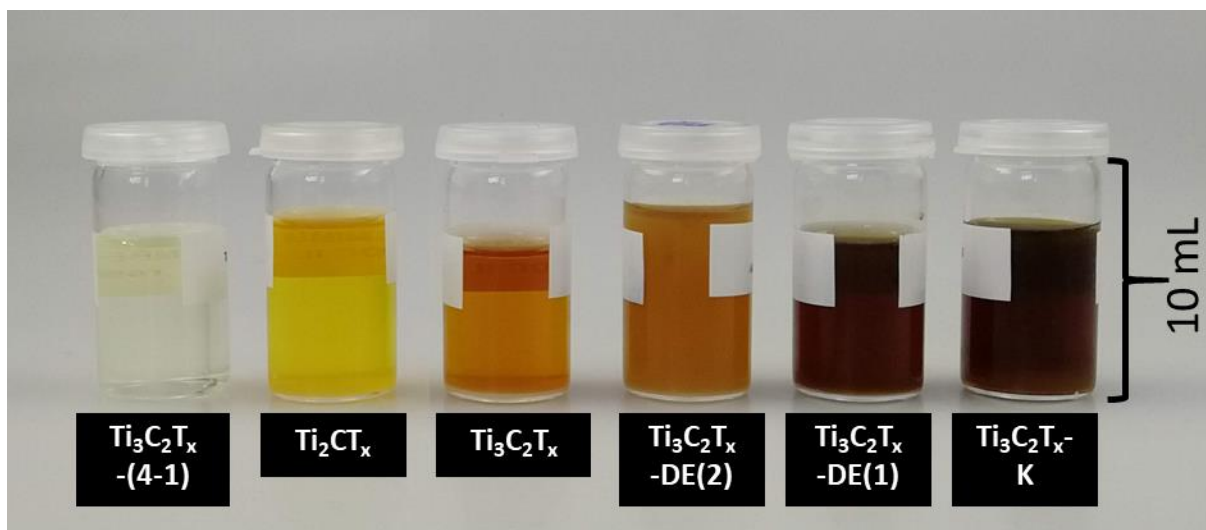


Figure S5: Ionic liquid residue after the etching process. $\text{Ti}_3\text{C}_2\text{T}_x\text{-DE(1)}$ and $\text{Ti}_3\text{C}_2\text{T}_x\text{-DE(2)}$ corresponds to first and second etching in the $\text{Ti}_3\text{C}_2\text{T}_x\text{-DE}$ sample.

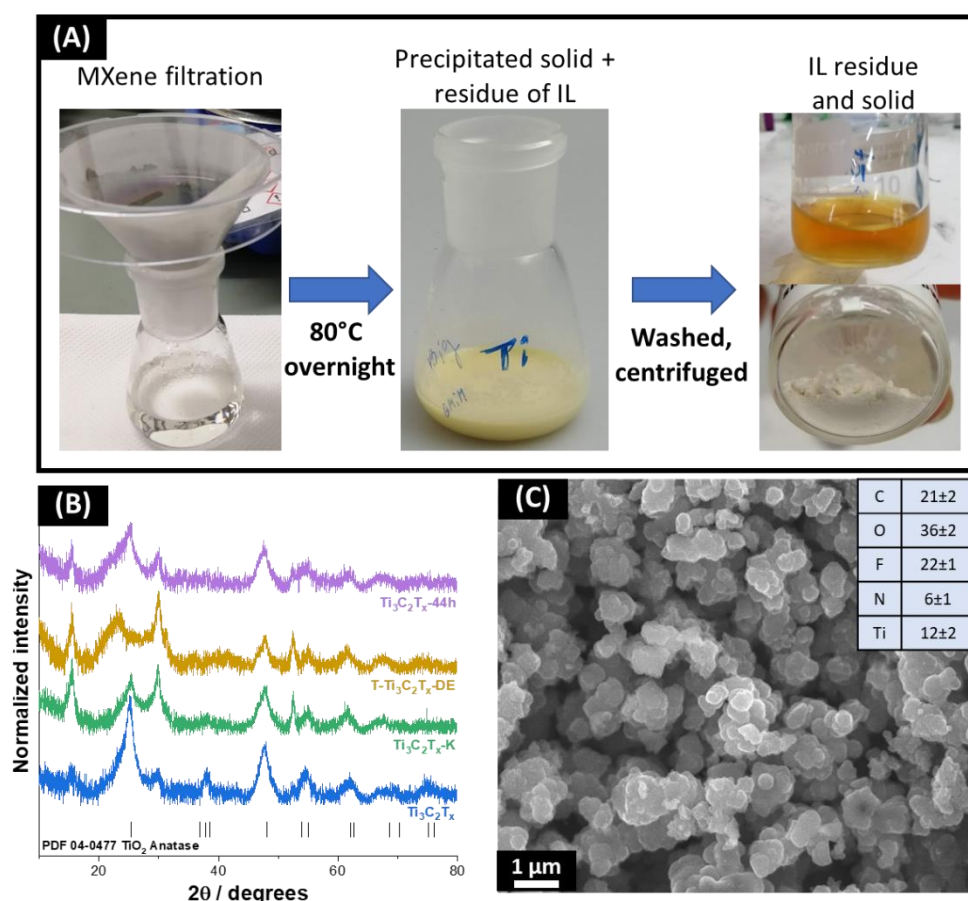


Figure S6: (A) Digital photographs of the steps of separation of IL residue and oxide forming during etching. (B) X-ray diffraction patterns from the powder separated from IL residue after filtration from the etched MAX phases. (C) Scanning electron micrograph with elemental data (in atomic %) of $\text{Ti}_3\text{C}_2\text{T}_x$ residue solid separated from the IL.

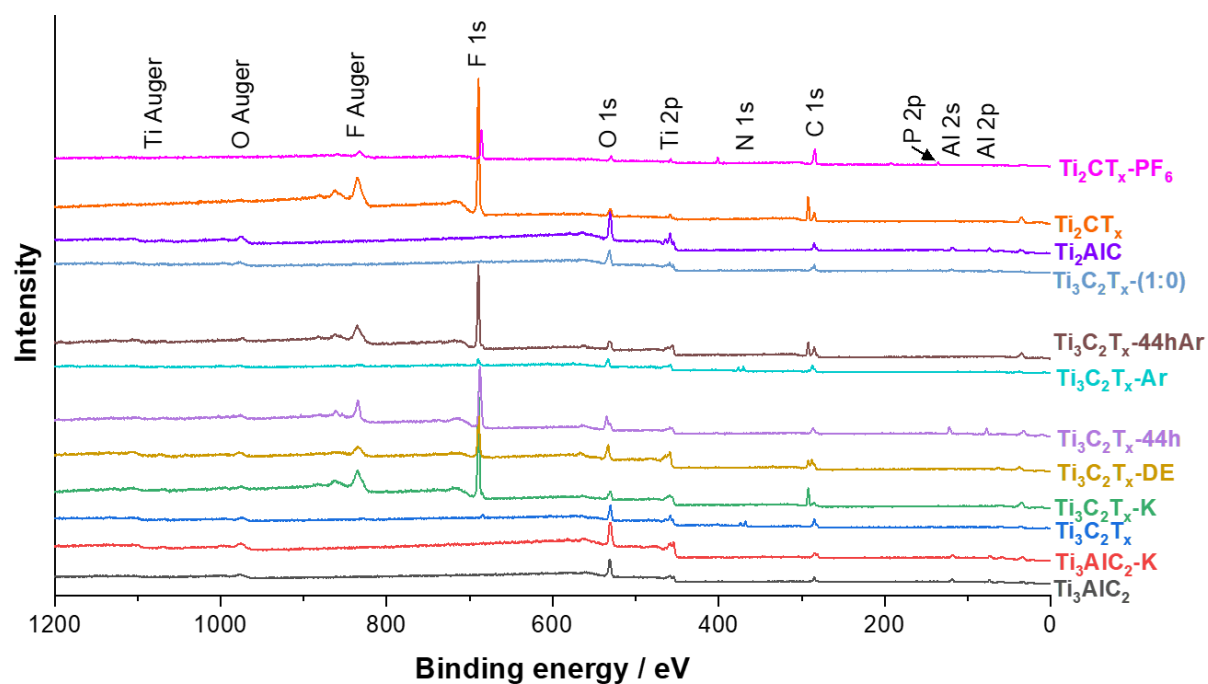


Figure S7: X-ray photoelectron survey spectra of the IL-etched MAX phases.

During delithiation, there is an increased current signature in the cyclic voltammogram of $\text{Ti}_3\text{C}_2\text{T}_x$ and $\text{Ti}_3\text{C}_2\text{T}_x\text{-HF}$; this feature is significantly depressed for sample $\text{Ti}_3\text{C}_2\text{T}_x\text{-K}$ (**Fig. 4A-B**). The latter also has a relatively poor rate handling ability (**Fig. 4C**) and this may delay the delithiation kinetics compared $\text{Ti}_3\text{C}_2\text{T}_x$, thereby, resulting in the absence of a clearly discernible peak at 0.3 V vs. Li/Li^+ . In the literature, the current peak at 0.01/0.3 V vs. Li/Li^+ has been assigned to lithium intercalation/deintercalation in MXene. The additional peak signature of $\text{Ti}_3\text{C}_2\text{T}_x\text{-HF}$ (**Fig. S10**) between 0.6-1.5 V vs. Li/Li^+ are in alignment with other HF-etched MXene samples.³ The differences seen in the first cycle between the samples may relate to the different surface terminations obtained from the different etching processes.

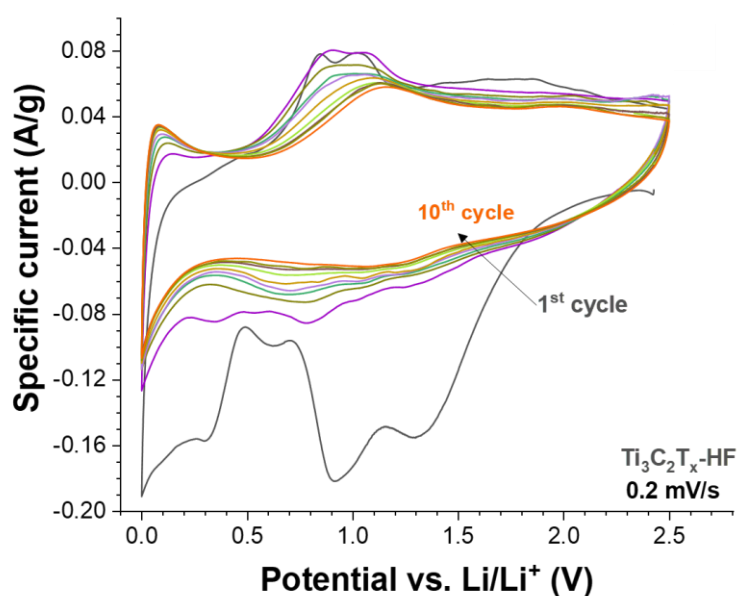


Figure S8: First 10 cyclic voltammograms at 0.2 mV/s of the HF-etched Ti_3AlC_2 . During the 1st cycle, the anodic scan peaks align with irreversible reactions related to the solid-electrolyte interface.

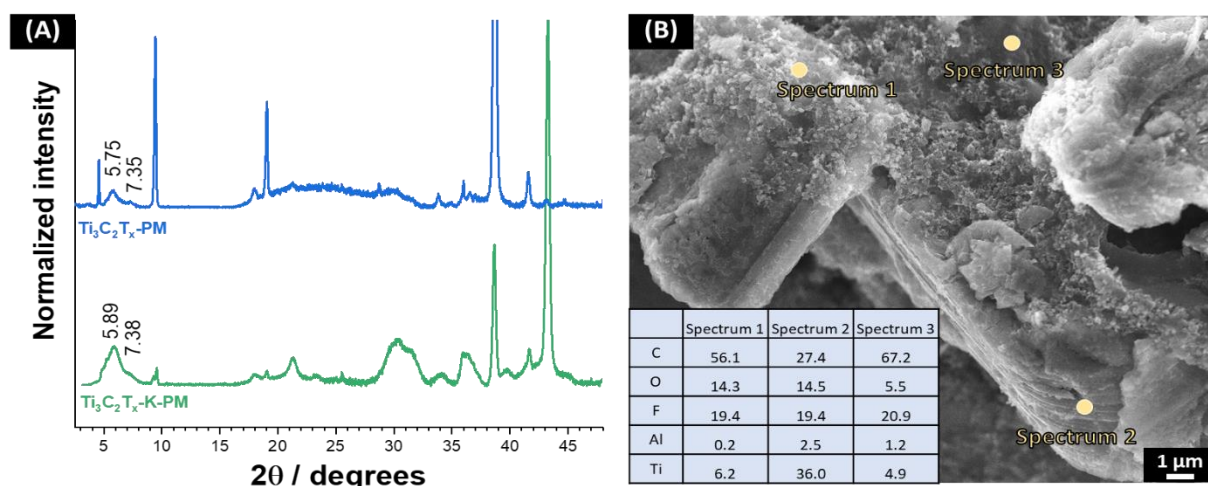


Figure S9: (A) X-ray diffraction patterns from the $\text{Ti}_3\text{C}_2\text{T}_x$ and $\text{Ti}_3\text{C}_2\text{T}_x\text{-K}$ electrodes after rate handling test (post mortem analysis). (B) Scanning electron micrograph with elemental data (in atomic %) of $\text{Ti}_3\text{C}_2\text{T}_x$ electrode after cycling. Spectrum 1, 2, and 3 correspond to regions with PVDF, MXene, and carbon, respectively.

Table S3: Interlayer spacing obtained from the (002) X-ray reflections.

Sample	<i>d</i> spacing / Å (reflection position)		
	I	II	III
Ti_3AlC_2			9.31 (9.50)
$\text{Ti}_3\text{AlC}_2\text{-K}$			9.21 (9.60)
$\text{Ti}_3\text{C}_2\text{T}_x$	23.03 (3.84)	13.85 (6.38)	9.36 (9.45)
$\text{Ti}_3\text{C}_2\text{T}_x\text{-K}$	23.18 (3.81)	13.43 (6.58)	9.39 (9.42)
$\text{Ti}_3\text{C}_2\text{T}_x\text{-DE}$	23.15 (3.82)	13.40 (6.60)	9.35 (9.46)
$\text{Ti}_3\text{C}_2\text{T}_x\text{-44h}$	25.68 (3.44)	13.51 (6.54)	9.43 (9.38)
$\text{Ti}_3\text{C}_2\text{T}_x\text{-Ar}$		13.56 (6.52)	9.32 (9.49)
$\text{Ti}_3\text{C}_2\text{T}_x\text{-44hAr}$	23.70 (3.73)	13.47 (6.56)	9.45 (9.36)
$\text{Ti}_3\text{C}_2\text{T}_x\text{-(1:0)}$			9.35 (9.46)
Ti_2AlC			6.87 (12.88)
$\text{Ti}_2\text{CT}_x\text{-PF}_6$		9.43 (9.37)	6.87 (12.89)
$\text{Ti}_3\text{C}_2\text{T}_x\text{-HF}$			10.21 (8.66)

Table S4: Comparison of different MAX etching methods and MXene characteristics. NA stands for “not available” and RT denotes “room temperature”.

MAX	Etching agent	Etching conditions	d-spacing (Å)	Functionalities/composition	Reference
Ti ₃ AlC ₂	EMIMBF ₄ /water ("Ionic liquid")	20 h, 80 °C	13.4-23.7	Ti ₃ Al _{0.1} C _{1.8} O _{1.2} F _{0.7} (EDX)	This work
Ti ₃ AlC ₂	HF 50%	2 h, RT	9.8	12%F, presence of OH Ti ₃ C ₂ (OH) _{0.12(2)} F _{0.8(2)} O _{0.54(7)}	4, 5
Ti ₃ AlC ₂	HF 5%	24 h, RT	9.8	Ti ₃ Al _{0.02} C _{1.36} O _{1.09} F _{1.04} (EDX)	6
Ti ₃ AlC ₂	LiF/HCl (6 M) ("in situ HF")	45 h, 40 °C	13.5-14	Ti ₃ C ₂ (OH) _{0.06(2)} F _{0.25(8)} O _{0.84(6)}	5, 7
Ti ₃ AlC ₂	LiF/HCl (9 M) ("in situ HF")	24 h, 35 °C	10-14	NA	8
Ti ₃ AlC ₂	1 M NH ₄ HF ₂	8 h, 60 °C	12.5	NA	9
Ti ₃ AlC ₂ film	1 M NH ₄ HF ₂	160 min to etch a 28 nm film	12.3	Ti ₃ C _{2.2} O ₂ F _{0.6} Ti ₃ C _{2.3} O _{1.2} F _{0.7} N _{0.2}	10
Ti ₃ AlC ₂	Hydrothermal NaOH ("alkali etching")	NaOH 27.5 M, Ar, 12 h, 270 °C	12	40.4at% O, 6.29at% Na (XPS) 45.5 mass% O, 3.1 mass% Na (XRF)	11
Ti ₃ AlC ₂	NH ₄ HF ₂ /PC ("water-free")	196 h, 35 °C Washing with HCl	13.5-21	Ti ₃ C _{1.26} O _{2.85} F _{7.2} (XPS) Functional. Terminations: 70% F, 30% -O/OH	12
Ti ₃ SnC ₂	CuCl ₂ molten salt ("fluorine-free")	24 h, 750 °C washing with ammonium persulfate	11.0	19.8 at% O, 16.5 at% Cl (EDX)	13
Ti ₃ AlC ₂	Electrochemical etching	0.3 V vs. RHE, 50 °C, 9 h	9.2	Ti ₃ Al _{0.77} C _{0.8} O _{0.22} (EDX)	14

Supporting References:

1. D. Weingarth, M. Zeiger, N. Jäckel, M. Aslan, G. Feng and V. Presser, *Advanced Energy Materials*, 2014, **4**, 1400316.
2. M. Widmaier, B. Krüner, N. Jäckel, M. Aslan, S. Fleischmann, C. Engel and V. Presser, *Journal of the Electrochemical Society*, 2016, **163**, A2956-A2964.
3. M. Naguib, J. Come, B. Dyatkin, V. Presser, P. L. Taberna, P. Simon, M. W. Barsoum and Y. Gogotsi, *Electrochemistry Communications*, 2012, **16**, 61-64.
4. M. Naguib, M. Kurtoglu, V. Presser, J. Lu, J. Niu, M. Heon, L. Hultman, Y. Gogotsi and M. W. Barsoum, *Advanced Materials*, 2011, **23**, 4248-4253.
5. M. A. Hope, A. C. Forse, K. J. Griffith, M. R. Lukatskaya, M. Ghidui, Y. Gogotsi and C. P. Grey, *Phys. Chem. Chem. Phys.*, 2016, **18**, 5099-5102.
6. M. Alhabeb, K. Maleski, B. Anasori, P. Lelyukh, L. Clark, S. Sin and Y. Gogotsi, *Chemistry of Materials*, 2017, **29**, 7633-7644.
7. M. Ghidui, M. R. Lukatskaya, M.-Q. Zhao, Y. Gogotsi and M. W. Barsoum, *Nature*, 2014, **516**, 78-81.
8. F. Shahzad, M. Alhabeb, C. B. Hatter, B. Anasori, S. M. Hong, C. M. Koo and Y. Gogotsi, *Science*, 2016, **353**, 1137-1140.
9. A. Feng, Y. Yu, F. Jiang, Y. Wang, L. Mi, Y. Yu and L. Song, *Ceramics International*, 2017, **43**, 6322-6328.
10. J. Halim, M. R. Lukatskaya, K. M. Cook, J. Lu, C. R. Smith, L.-Å. Näslund, S. J. May, L. Hultman, Y. Gogotsi and P. Eklund, *Chemistry of Materials*, 2014, **26**, 2374-2381.
11. T. Li, L. Yao, Q. Liu, J. Gu, R. Luo, J. Li, X. Yan, W. Wang, P. Liu and B. Chen, *Angewandte Chemie International Edition*, 2018, **57**, 6115-6119.
12. V. Natu, R. Pai, M. Sokol, M. Carey, V. Kalra and M. W. Barsoum, *Chem*, 2020.
13. Y. Li, H. Shao, Z. Lin, J. Lu, L. Liu, B. Duployer, P. O. Persson, P. Eklund, L. Hultman and M. Li, *Nat. Mater.*, 2020, 1-6.
14. S.-Y. Pang, Y.-T. Wong, S. Yuan, Y. Liu, M.-K. Tsang, Z. Yang, H. Huang, W.-T. Wong and J. Hao, *Journal of the American Chemical Society*, 2019, **141**, 9610-9616.